

Optimizing the froth area of large mechanical flotation cells

Rodrigo Grau¹, Diego Davoise², Alejandro Yáñez¹, Ángel López²

1. *Outotec Finland*

2. *Proyecto Riotinto Atalaya Mining, Spain*

ABSTRACT

A flotation cell can be divided into two distinctive zones: the collection zone and the froth zone. Each zone plays a fundamental role in the flotation process; in the collection zone, slurry is mixed and solids are kept in suspension; air is dispersed into small flotation bubbles, and particles are collected by the small bubbles and carried to the froth phase. In a flotation cell, an efficient collection zone is achieved by selecting an adequate mixing rotor-stator mechanism in terms of size and operating velocity. The flotation cell design should also provide a suitable environment for creating a stable froth that can easily overflow from the launder lip of the cell.

Froth removal in flotation can be affected by modifying the open froth area in the flotation cell, so that the modification has a direct effect on the metallurgical performance of the flotation cell. The effect of reducing the open froth area was evaluated in a large flotation cell, TankCell® e300, in operation at a copper concentrator. The froth area was drastically reduced by installing a new set of concentrate launders. This paper contains a detailed description of the evaluation of the new concentrate launder. The metallurgical performance of the cell was evaluated before and after the installation of the launder.

INTRODUCTION

In flotation, hydrophobic particles are collected and carried by air bubbles from a liquid-solids suspension (slurry) to a froth phase, which has been stabilized with chemical agents known as frothers, whereas hydrophilic particles remain uncollected in the liquid-solids suspension. The material flow in the flotation process is illustrated in Figure 1 (Yianatos, 2005). It is clear from this diagram that many complex subprocesses take place in the flotation process. In a flotation cell, the rotor-stator mechanism should mix the solids particles and keep them in suspension while dispersing air into fine bubbles throughout the complete volume of the flotation cell. The mixing should be turbulent enough to create the possibility of bubble particle collection, balancing the attachment and detachment of bubbles and particles while also allowing the generation of a zone for stable froth formation. The froth should be sufficiently stable for the collected particles to report to the concentrate launder. In the froth phase, bubbles come close enough to each other to coalesce, releasing the hydrophobic particles and interstitial water, and the majority of the hydrophobic particles remain and reattach to the bubble surface in the froth while the less hydrophobic particles

such as mixed and large grains may drop back to the slurry phase (Heath and Runge, 2019). Another key function of the froth is to reduce the entrainment of gangue material. There exist two mechanisms by which particles are carried to the froth phase: true flotation and entrainment. Entrainment is a non-selective process and therefore has a detrimental effect on the concentrate grade (Kracht et al., 2016). It is also well known that particles in the froth phase contribute to the stability of the froth phase; in fact, froth recovery has found to be affected by the particle size, and the presence of fine particles has a positive effect on froth recovery (Rahman et al., 2012). Therefore, froth stability decreases as the number of particles in the froth decreases. This is a phenomenon that can be easily observed in the rougher stage. The first flotation cells in the rougher stage can be operated with deep and stable froths while the froth in the last cells is brittle and shallow and it is difficult for the froth to flow over the lip of the cell.

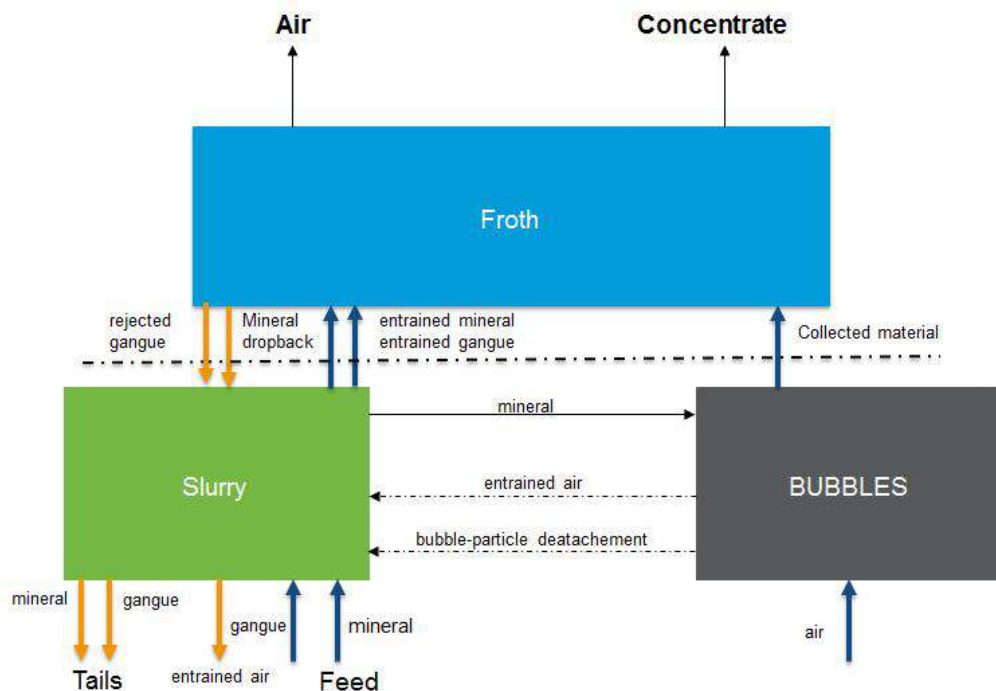


Figure 1 Schematic diagram of the main material flows in the flotation process.

The froth recovery factor was introduced by Finch and Dobby (1990) for froth columns. Froth recovery is defined as the fraction of particles entering the froth phase by true flotation (attached to bubbles) that are recovered via the concentrate launder, describing the overall recovery of floatable minerals as in Equation 1:

$$R_G = \frac{R_c R_f}{1 - R_c (1 - R_f)} \quad (1)$$

where R_G is the overall recovery and R_f is the froth recovery and R_c is the collection zone recovery, the overall recovery calculation is shown schematically in Figure 2.

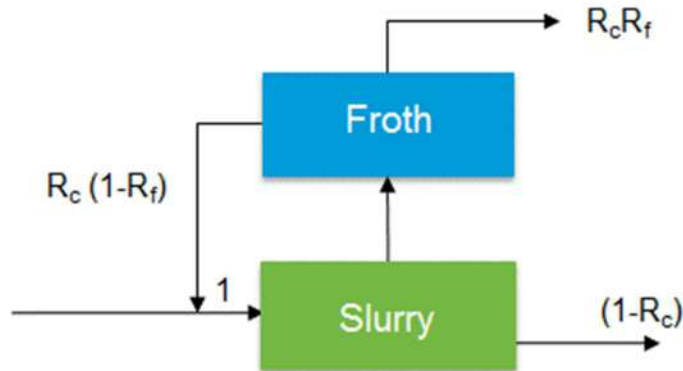


Figure 2 Model for the overall recovery based on collection and froth zone.

Froth recovery is a complex measurement and several techniques have been developed to determine it (Runge et al., 2010). Froth recovery has been reported to vary over a wide range: Savassi et al. (1997) found that froth recovery in Pb rougher flotation dropped from 70% in the first cell to 10% in the last cells of the bank. Yianatos et al. (2008) reported a froth recovery of 66 % for the first cell of a Cu rougher bank into a 130 m³ mechanical flotation cell.

NEW CONCENTRATE LAUNDER WITH ADJUSTABLE FROTH CROWDER

Froth crowders are used to decrease the Froth Surface Area (FSA) of a flotation cell, enhancing the movement of the froth to launders. The FSA is modified in a flotation cell by the type of crowder and launder selected for the flotation cell. A set of commonly available of flotation launders for large flotation cells is presented in Figure 3 (Grau, 2016, Heath, 2016 and Heath and Runge, 2019); in addition, radial launders can be used with the launder types shown in the figure below. Froth crowders in combination with the launder design are used to enhance and ensure adequate froth recovery.

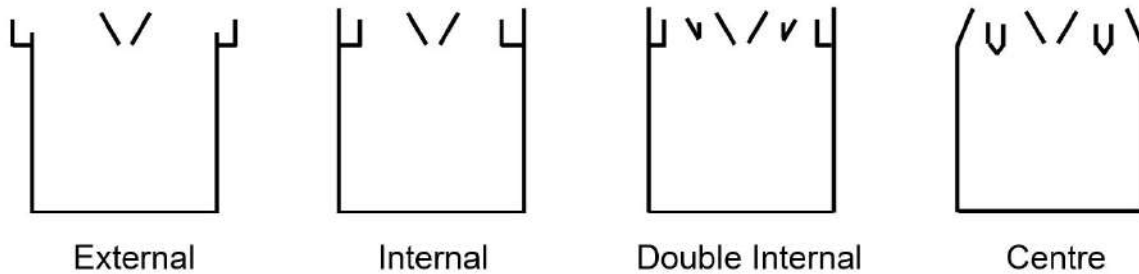


Figure 3 Type of flotation cell launders available for large flotation cells.

An adjustable froth crowder and new center launder were installed in an existing TankCell® e300 equipped with an internal peripheral launder (see Figure 3, second configuration from the left). The adjustable froth crowder is depicted in Figure 4; the position of the additional crowdors can be modified by using a screw jack type of lifting mechanism equipped with electrical actuators. The new combination of crowder and concentrate launder drastically modified the FSA of the cell without significantly modifying the effective volume of the cell. The level of crowding (CL) is given in Table 1 and is calculated according to Equation 2:

$$CL = 100 \left(\frac{TSA - FSA}{TSA} \right) \quad (2)$$

where TSA corresponds to the main Tank Surface Area at the bottom of the flotation cell. In addition, the distance that the particle travels from the froth to the lip of the collection launder is significantly reduced and has been reported to have an impact on froth recovery and the overall performance of flotation equipment (Contreras et al. 2013, Vallejos et al., 2018). Furthermore, an increase in lip length is provided by the new symmetrical design.

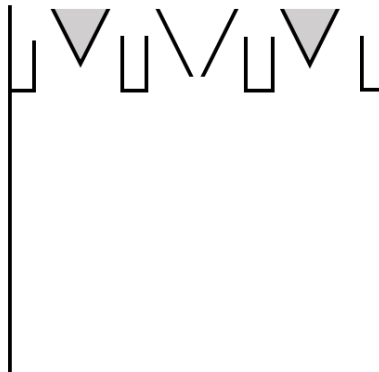


Figure 4 Adjustable froth crowder with an additional crowder, shown in gray; the position is adjustable.

Table 1 Crowding level for two different concentrate launder setups

	Original Internal Launder	Upgrade 2018 Adjustable Crowder
Nominal Volume	300	300
Level of Crowding (CL)	29.2	76.1

ATALAYA MINING PROYECTO RIOTINTO

A new set of concentrate launders was installed in the first cell of a rougher bank of four flotation units at the Atalaya Mining Proyecto Riotinto copper concentrator. The Proyecto Riotinto is an open-pit copper mine located in Andalucía, Spain. Commercial production of copper concentrates began after the refurbishment of the concentrator plant in February 2016. During the refurbishment, five Outotec TankCells were installed. Three TankCell e100 units equipped with center launders in a configuration of 1+1+1 were installed for rougher duty, and two TankCell 100 HG (High Grade) units in a configuration of 1+1 were installed in the cleaner stage.

A TankCell e300 was installed and commissioned at the end of 2016 as part of the plant optimization project. The larger cell was installed as the first cell of the existing rougher bank; thus the new rougher bank consisted of four flotation cells with a total nominal volume of 600 m³ in a configuration of 1+1+1+1, as illustrated in Figure 5.

The installation of the new adjustable crowder and center launder was carried out during a plant shutdown at the end of July 2018. The main aim of the concentrate launder upgrade was to improve the performance of the cell and therefore to improve the metallurgical performance of the rougher bank.

The main operating parameters of the rougher stage are given in Table 2: the overall conditions in the table are the monthly average from May to December 2018, the original condition is from May until July 2018, and the new launder condition is from August to December 2018.

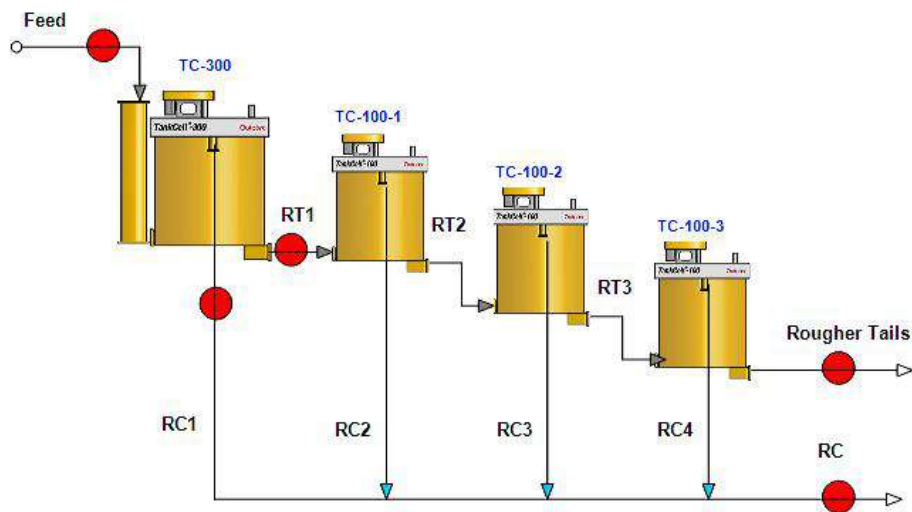


Figure 5 Rougher bank TankCell 300 + 3 TankCell 100 units. The red points indicate the sampled streams.

Table 2 Main operating conditions, monthly average from May 2018 to January 2018

	Overall	Original Launder	New Launder
P80, μm	190	180	198
Cu head grade, %	0.46	0.42	0.49
Tonnage, t/h	1196	1196	1196
Pulp solids content, %	40.5	39.8	41.2

OPERATING PARAMETERS

After the installation of the new concentrate launder with the adjustable crowder, new operating conditions were defined for the new technology; this initial stage was defined as the optimization phase. During the optimization work, it was determined how the cell should be operated to maximize the recovery of the flotation cell. In consultation with the plant personnel it was decided that an acceptable concentrate range for this cell should be between 5 to 10% Cu grade, since this is a rougher cell and the main target for this cell is to reach as high recovery as possible. In the optimization phase, the effect of the air flow rate, froth depth, and the position of the crowder was varied. The most drastic change was observed in the amount of air required in order for the froth to continuously flow over the lip of the flotation cell. This can be clearly observed in Figure 6. During August, the amount of air fed to the cell was decreased from over 35 m³/min to values below 20 m³/min nearer September. It should be mentioned that after the installation of the new technology, all the stagnant froth zones had disappeared. This was verified by a research team from the Imperial College using special froth cameras. Furthermore, it was concluded that the air recovery (Neethling and Cilliers, 2008) was higher for the new concentrate launder (Brito-Parada et al., 2019).

Table 3 Average operating conditions of the TankCell 300

	Original Launder		New Launder	
	Average	Standard deviation	Average	Standard deviation
Air flow, m ³ /min	37	2.7	22.6	5.1
Froth depth, cm	13		16	3.9
Position of the adjustable crowder			Lowest	

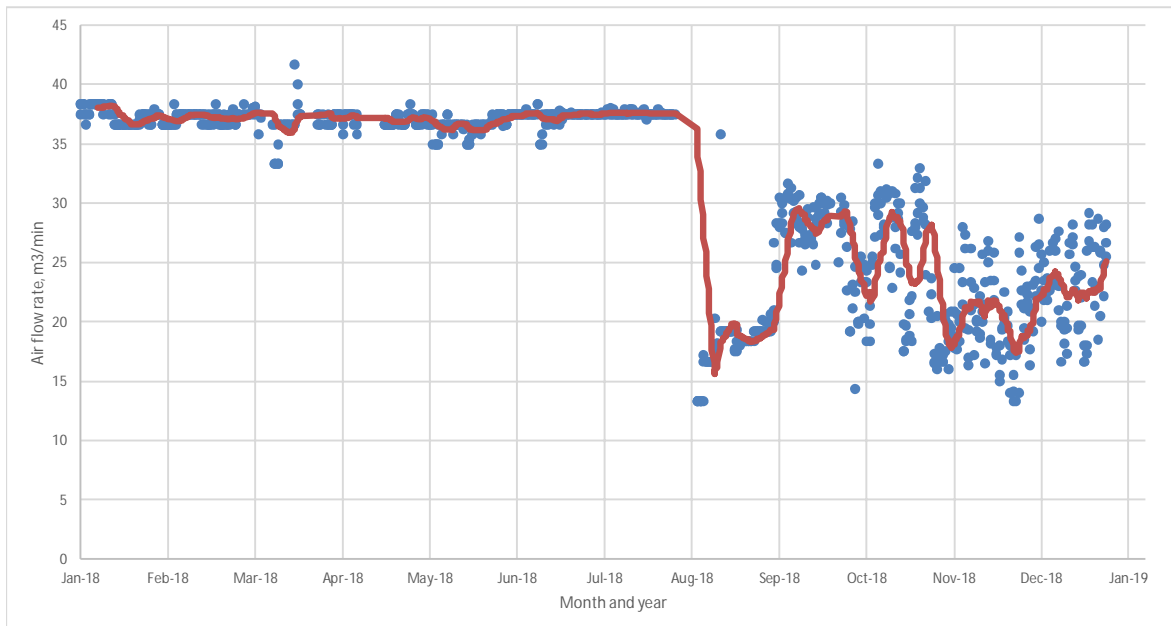


Figure 6 Change in air flow rate over time, before and after installation of new froth launder. Launder installed end of July.

METALLURGICAL RESULTS

Samples are taken from the rougher circuit as shown in Figure 5. The samples are collected either manually or using automatic samplers. Three shift composite samples are collected for each stream per day. In the case of the RC1 stream, the sample is manually collected every two hours and shift composite samples are prepared. The sampled streams and type of sampling are shown in Table 4.

Table 4 Sampled streams

Stream	Type of sampler
Fresh feed, feed	Gravity sampler
TankCell e300 concentrate, RC1	Manual
TankCell e300 tails, RT1	Gravity sampler
Rougher concentrate, RC	Pressure pipe sampler
Rougher tails	Gravity sampler

Daily Cu grades and recoveries are calculated by weighing the shift recoveries by the tonnage processed during the corresponding shift; thus the monthly Cu recovery is then calculated based on daily Cu recoveries. The recoveries reported in this work are monthly recoveries and grades. The recoveries achieved by the TankCell 300 flotation cell are tabulated in Table 5 and plotted in Figure 7 and 8.

It is clear from the metallurgical results that, by changing the launder type, the performance of the cell improved from 59% Cu recovery to values above 67%, reaching 69.9 % during December 2018. The authors postulate that the metallurgical performance improvement is mainly due to a drastic increase in froth recovery. According to the model developed by Vallejos et al. (2019), there seems to be an indication that the froth recovery increased from 45 % to values above 85%. The decrease of the Cu grade in the concentrate (see Table 6) is also a clear indication that the froth recovery had increased; the increase in froth recovery resulted in an increased recovery of water as well as gangue entrainment in the flotation cell. Hence, the introduction of the new technology improved the metallurgical performance of the rougher stage. Both the regrinding and the cleaner flotation circuit had sufficient capacity to process the increment in rougher concentrate flow rates, thus the gain in the rougher stage was exploited to boost overall plant performance.

Another important consideration is that the recovery increased even though the amount of flotation air was drastically reduced. This seems to indicate that the collection zone in the flotation cell is equally efficient at lower air flow rates. Therefore, one can conclude that the excess of air is only used to stabilize the froth and promote its movement to the lip of the flotation cell.

Table 5 Cu Recovery for the TankCell-300 unit, before and after modification (Jan only until 21.01)

	Before Installation			Optimization phase			After Installation		
	May	June	July	Aug	Sep	Oct	Nov	Dec	Jan
Cu recovery, %	59.4	58.6	59.1	61.5	67.8	61.8	69.0	69.9	67.2
Cu recovery, %	59.0			63.7			68.7		

Table 6 Cu concentrate grade in TankCell-300 flotation cell, before and after modification

	Before Installation			Optimization phase			After Installation		
	May	June	July	Aug	Sep	Oct	Nov	Dec	Jan
Cu grade, %	17.1	21.2	20.1	21.0	13.6	13.7	10.8	11.4	13.9
Cu grade, %	19.4			15.7			11.8		

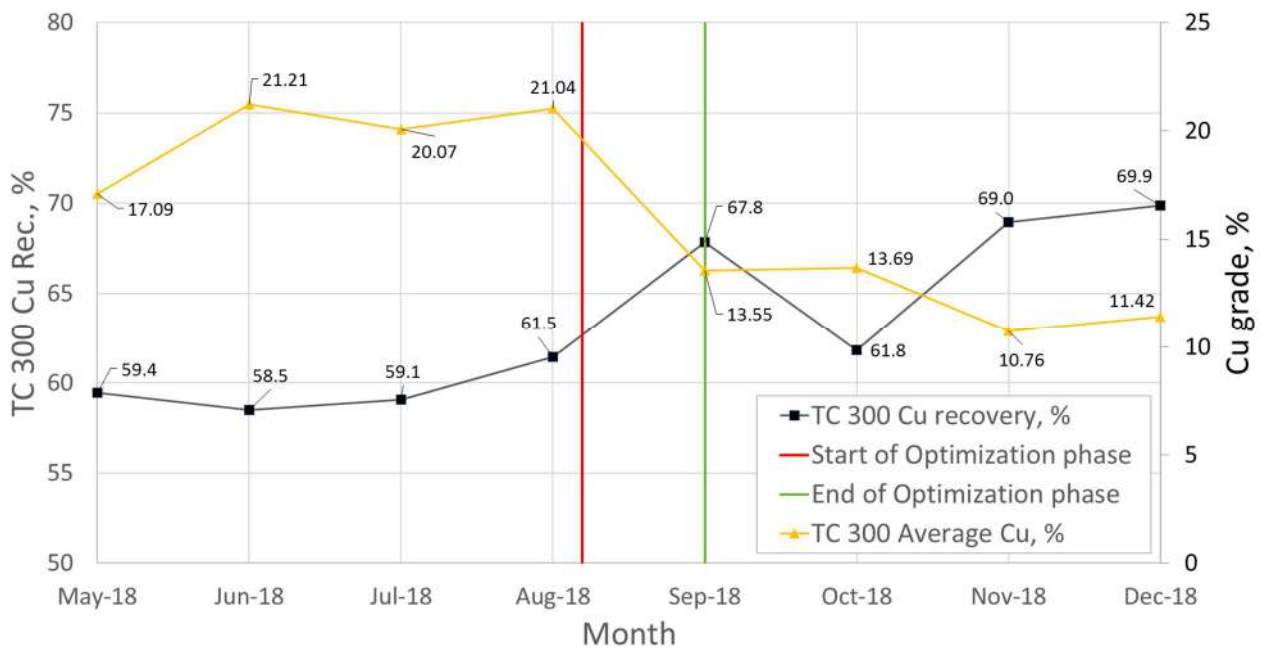


Figure 7 Impact of the launder upgrade on the performance of the flotation cell.

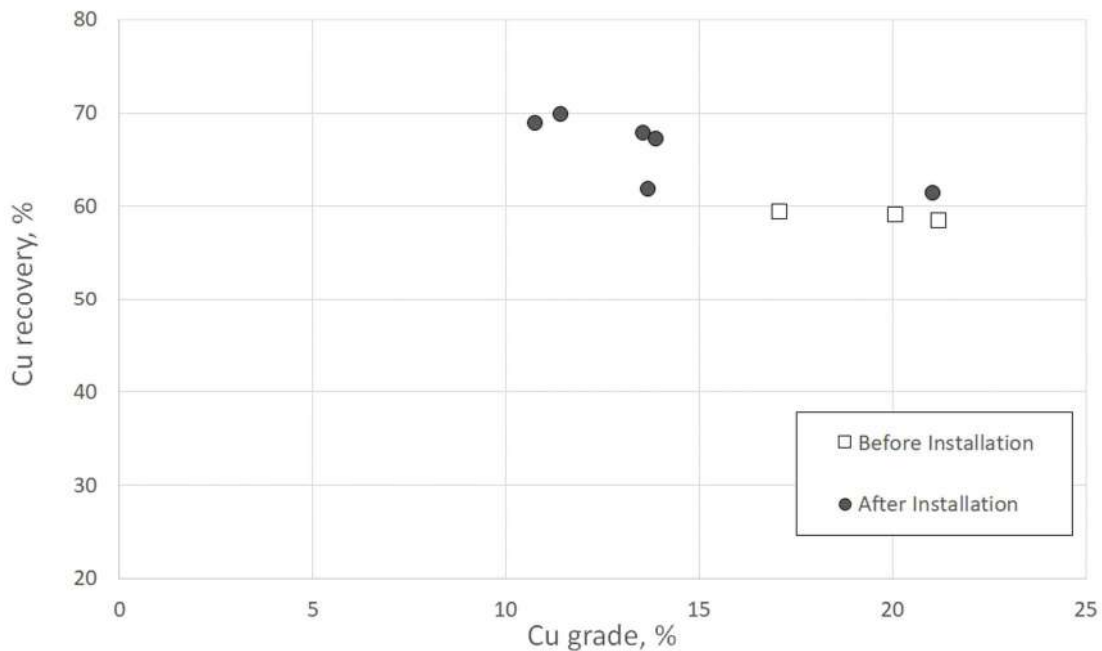


Figure 8 Cu recovery vs. grade curve, monthly average for the 8 months of operation.

CONCLUSION

The following conclusions can be drawn from the implementation of the new technology:

- A new concentrate launder with an adjustable froth crowder was developed and installed in a TankCell® e300 operating in the rougher stage in a copper concentrator.
- The change of concentrate launder drastically reduced the froth surface area and increased the lip length, resulting in a reduction of the distance that the collected particles travel to the concentrate lip.
- The use of the new technology resulted in better froth stability; higher froth velocities and stagnant zones in the froth were completely eliminated.

- The new concentrate launder allowed a significant reduction in the air fed to the flotation cell.
- An important increase in Cu recovery was observed in the flotation cell; the recovery increased from 59% to values above 68% for the individual cell working as the first cell in the rougher stage.
- It was demonstrated that the metallurgical performance could be affected by optimizing the froth area in the mechanical flotation cell.

ACKNOWLEDGEMENTS

The authors of this paper would like to acknowledge all the people that have participated in the design, installation, and optimization of this new launder. We would also like to thank the metallurgical laboratory at Atalaya Mining for their great work and of course we would like to thank Atalaya Mining Management for allowing us to publish this paper.

REFERENCES

Brito-Parada, P., Mesa, D. Quintanilla, P. (2019) 'Report on TC300 Launder Design Evaluation at Atalaya Mining's Riotinto Project'.

Contreras, F. Yianatos, J, Vinnett, L. (2013) 'On the froth transport modelling in industrial flotation cells', *Minerals Engineering*, Volume 41, pp. 17-24.

Finch, J. Dobby G. (1990) '*Column Flotation*' (first ed.), Pergamon Press, London, UK.

Grau, R. /Outotec (2016) Outotec Webinars for Mining, Metals and Energy Professionals, Optimización del área de espuma en la celda de flotación. 10.7.2019. <http://www.outotec.com/Webinars>.

Heath, J. /Outotec (2016) Outotec Webinars for Mining, Metals and Energy Professionals, Optimizing froth area of the flotation cell. 10.7.2019. <http://www.outotec.com/Webinars>

Heath, J. Runge, K. (2019) *SME Mineral Processing & Extractive Metallurgy Handbook*, Society for Mining, Metallurgy & Exploration. USA.

Kracht, W. Orozco, Y. Acuña, C. (2016) 'Effect of surfactant type on the entrainment factor and selectivity of flotation at laboratory scale', *Minerals Engineering*, Volume 92, 216-220.

Neethling, S. Cilliers, J. (2008) 'Predicting air recovery in flotation cells' *Minerals Engineering*, Volume 21, Issues 12–14, pp. 937-943.

Rahman, R. Ata, S. Jameson, G. (2012) 'The effect of flotation variables on the recovery of different particle size fractions in the froth and the pulp', *International Journal of Mineral Processing*, Volumes 106–109, Pages 70-77.

Runge, K. Crosbie, R. Rivett, T. McMaster, J. (2010) 'An Evaluation of Froth Recovery Measurement Techniques' *XXV International Mineral Processing Congress (IMPC) Proceedings, Brisbane 6-10 September*, pp. 2313-2324.

Savassi, O. Alexander, Johnson, N. Franzidis, J. Manlapig, E. (1997) 'Measurement of Froth Recovery of Attached Particles in Industrial Flotation Cells', *in Proceedings of the Sixth Mill Operator's Conference*, pp. 149-155.

Vallejos, P. Yianatos, J. Matamoros, C. and Díaz, F. (2019) 'Mineral Solids Transport in a Two Dimensional Flotation Froth', *Minerals Engineering*, Volume 138, pp. 24-30.

Vallejos, P. Yianatos, J. Grau, R. Yáñez, A. (2019) 'Evaluation of New Flotation Circuits Design', *submitted to Flotation 2019*.

Yianatos, J. (2005) '*Flotación de Minerales*', Universidad Técnica Federico Santa María, Valparaíso, Chile.

Yianatos, J. Moys, M. Contreras, F. Villanueva, A. (2008) 'Froth recovery of industrial flotation cells', *Minerals Engineering*, Volume 21, Issues 12-14, pp. 817-825.